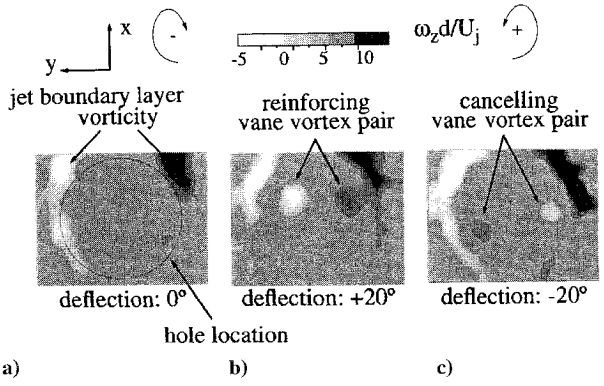

Fig. 4 Time-averaged PIV vorticity plots in x–y plane for BR = 1.6 and z/d = 0.13. Black and white regions indicate positive and negative vorticity, respectively. The gray regions indicate vorticity that is near zero.

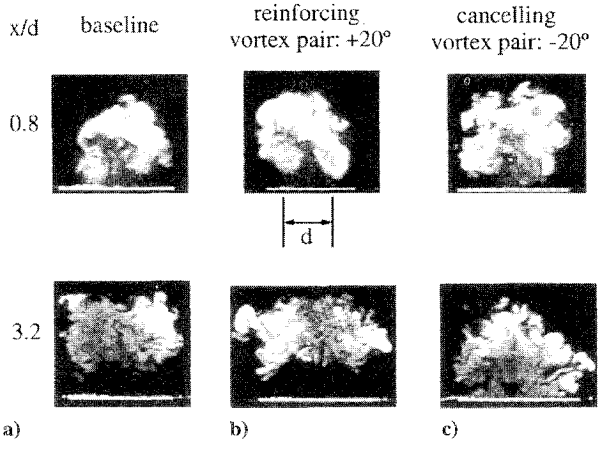

Fig. 5 Jet cross sections in the y–z plane (BR = 1.6) for vane deflections of 0, +20, and −20 deg. The hole trailing edge is located at x/d = 0.

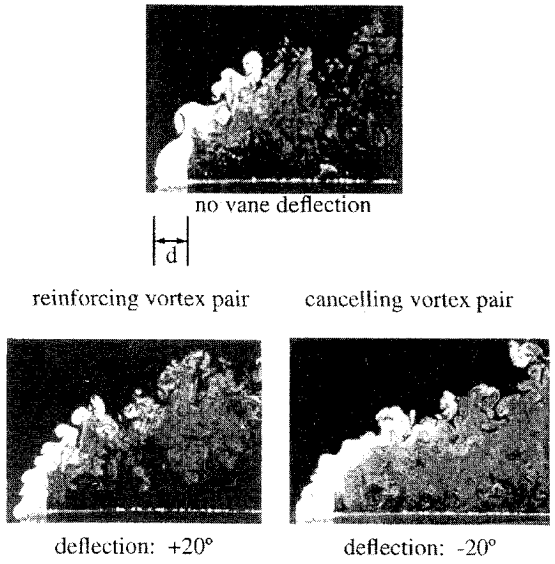

Fig. 6 Jet trajectory along centerline in x–z plane for vane deflections of 0, +20, and −20 deg and BR = 1.6.

vorticity and induces a z component of vorticity at the exit plane.[1] By placing a laser sheet at the jet exit in the x–y plane, this z component of vorticity becomes evident along the sides of the hole (see Figs. 4a–4c).

Figures 4b and 4c show that near the center of the hole a counter-rotating vortex pair is generated by the vanes. The rotational sense of this pair, determined by the direction of the vane deflection, is reversed between Figs. 4b and 4c.

Now that both kinds of vorticity are partially aligned at the hole exit plane, they can begin to reinforce or to cancel each other. Further downstream of the hole, the jet vorticity is convected by the jet and turned toward the x direction and becomes the conventional kidney vortices (w_x, $-w_x$) in the y–z plane of Fig. 1. The vane vortices are likewise transported along the jet trajectory and show up in the y–z plane as either a canceling ($-w_x$, w_x) or reinforcing (w_x, $-w_x$) vortex pair. This is the very place where the interaction of the two kinds of vortices becomes visible.

This appears to be the reason why the jet cross sections of Fig. 5c show better attachment further downstream of the hole for the canceling vortex pair, as compared with the reinforcing vortex pair of Fig. 5b. This trend is also seen in the jet trajectory views of Fig. 6.

III. Conclusions

The kidney-shaped vortices formed by a jet in a crossflow, which promote jet liftoff, can be weakened by introducing a canceling vortex pair into the jet prior to the hole exit. Even for a jet that is completely detached from the surface, the cancellation of the kidney vortices causes the jet to reside closer to the plate surface.

Acknowledgment

The financial support by U.S. Air Force Office of Scientific Research Grant F49620-95-1-0273, which is technically managed by Jim McMichael, is gratefully acknowledged.

References

[1]Haven, B. A., "The Effect of Hole Geometry on the Near Field Character of Crossflow Jets," Ph.D. Thesis, Dept. of Aeronautics and Astronautics, Univ. of Washington, Seattle, WA, 1996.

[2]Haven, B. A., and Kurosaka, M., "The Effect of Hole Geometry on Lift-Off Behavior of Coolant Jets," AIAA Paper 96-0618, Jan. 1996.

Multiple-Source Schlieren Noise Reduction Measurements

Terry Ray Salyer* and Steven H. Collicott†
Purdue University, West Lafayette, Indiana 47907-1282

Introduction

THE image produced by a schlieren system highlights gradients in air density which occur between the source slit and the knife edge, including inside the test section. The practice of verifying system alignment by observing the warm convective flow from one's hand is an example of the sensitivity to density gradients outside of the test section. Expansion of a flow to hypersonic Mach numbers leads to a lower static density than does expansion to supersonic Mach number. This low density, in conjunction with how the shock angles on relevant aerodynamic bodies at hypersonic speeds approach the Mach angle, leads to small density changes in the flow. Thus, density gradients outside of the test section (e.g., thermal currents from cooling of equipment) may be comparable in magnitude, yet are considered to be noise in the desired image. Minimizing these spurious density gradients is one step to alleviating image noise problems, with locating the schlieren system in an evacuated tank as the extreme case. Multiple-source schlieren modifications to existing systems has been shown be another, albeit unquantified, solution.[1] The present research quantifies system performance, supporting the previous theory. In addition, new nonaerodynamic

Presented as Paper 94-0279 at the AIAA 32nd Aerospace Sciences Meeting, Reno, NV, Jan. 10–13, 1994; received May 30, 1995; revision received April 19, 1996; accepted for publication July 23, 1996; also published in *AIAA Journal on Disc*, Volume 2, Number 1.

*Graduate Research Assistant, School of Aeronautics and Astronautics. Student Member AIAA.

†Associate Professor, School of Aeronautics and Astronautics. Senior Member AIAA.

applications of the multiple-source schlieren design[2] may also benefit from the quantified performance comparisons.

For 50 years people have demonstrated the multiple-source schlieren design,[3–9] yet the performance of the design, relative to a comparable system with a single source, has remained unquantified. Recent analysis by the authors[1,10] determines the parameters that describe the noise reduction properties of the system. Verification, be it qualitative or quantitative, of the performance of multiple-source schlieren systems relative to a single-slit system is lacking in the archival record. To address this shortage, data are acquired and analyzed for a variety of grid configurations and a noise-producing mask inserted between the two main mirrors. The measurement of such noise reduction, presented subsequently, enables the design of multiple-source schlieren systems with desired performance. Comparison of images (available in Ref. 10) provides a qualitative verification to complement the quantitative verification presented here.

Experiment

The multiple-source schlieren system used is of the standard Z-formation type commonly used with mirrored systems. The two collimation mirrors are f/10 spherical with 1.5-m focal lengths, separated by 3.75 m. The source and cutoff grids are positioned one focal length from their respective mirrors, and are approximately 5 deg off axis. Attached to and in front of the source grid is a ground glass plate that disperses the light from each slit. Following the cutoff grid, a pair of achromatic doublets forms the final image onto the charge-coupled device (CCD) camera. The object in the steady Mach 2.5 flow is a wedge with 11-deg half-angle. Images of the test region are acquired with a CCD array camera, recorded on videotape (S-VHS), and then digitized on an 8-bit gray scale over 768 × 493 pixels. To ensure that all images have approximately the same mean intensity, the automatic gain control on the camera is used.

Two regions of the images are analyzed: a 128 × 128 pixel area of undisturbed flow and the oblique shock wave. These are selected because they bound the density gradients in the flow; the uniform region has zero gradient, and the shock is essentially a discontinuity on the length scale of the imaging resolution. To measure the noise reduction capabilities of the system, a repeatable method of introducing spurious phase disturbances is required. This is performed with a speckle phase mask that simulates the presence of thermal currents (see Ref. 10). The speckle size used in the present work is 3 mm.

For a parametric study of the response of the multiple-source schlieren system to spurious density gradients at differing locations outside the test section, data are acquired for four grid configurations, all with cutoff edges parallel with the mean flow direction. The configurations used are as follows: single slit (L1), three-slit narrow spacing (L3N), three-slit wide spacing (L3W), and five slit (L5). All slits are 1.6 mm high, 12.7 mm long, and 6.35 mm apart, except for the three-slit wide grid (L3W), which are 12.7 mm apart. The single-slit case is a conventional schlieren system and, therefore, unambiguous and quantitative evaluation of the magnitude of sharp-focusing effects is possible with the results.[10]

Results

The radius of gyration of the histograms of the pixel gray-scale values are used to quantify the results in the 128 × 128 pixel region of uniform flow

$$r = \frac{1}{128}\sqrt{\sum_{I=0}^{255} n(I-\bar{I})^2} \qquad (1)$$

Fourier methods including power spectral densities, autocorrelations, and cross correlations were also applied, yet these methods failed to document the observable differences between images as well as the histogram method does.

For an image with high noise content, the overall range of pixel gray-scale values is large and covers most of the 8-bit gray scale, whereas the histogram of an image with low noise content is peaked. Thus, the radii of gyration computed for the images of lower noise levels are less than for the higher noise images. The histograms in Fig. 1 show this effect for the single-slit (L1) and five-slit (L5) systems with the phase mask at the 0 and 10% locations between the test section and mirror. The shaded region in each histogram marks the region one radius of gyration to either side of the mean intensity of that histogram. Note the differences between the 0 and 10% cases of the five-slit grid, and the lack of difference between 0 and 10% cases of the single-slit grid. This demonstrates that the five-slit grid is less sensitive to density gradients outside of the wind tunnel than the single-slit grid. Such measurements are repeated for spurious density gradients, simulated by the speckle phase mask, located throughout the region from test section to main mirror. This results in Fig. 2, which shows, through the radius of gyration, how the sensitivity to spurious density gradients decreases for gradients located farther away from the test section. Note that the single-slit system (L1) has the worst performance and the five-slit system (L5) has the best performance. It is worth noting that the three-slit narrowly spaced grid (L3N) performs better than the three-slit widely spaced grid (L3W). With the three-slit widely spaced system, it is expected that the response to spurious density gradients should drop off more quickly than the rest due to its shorter integration length. But this is not the case, which indicates that the widely spaced slits are less effective at reducing noise in this particular system. The similarity between the performance of the five-slit grid (L5) and the three-slit narrowly spaced grid (L3N) is another indication of the poor performance of the outermost slits from the axis. The poor performance of the outer slits is likely due to the aberrations of the system.[11]

The single-slit (L1) curve in Fig. 2 demonstrates the noise reduction capability present because of the long dimension of the source slit. This affects image structure in only one transverse dimension, and multiple slits are required to reduce noise with structure in the other direction. Note that extension of the concept of a long slit to two dimensions, i.e., a large square source, fails because it will have minimal sensitivity as a schlieren system.

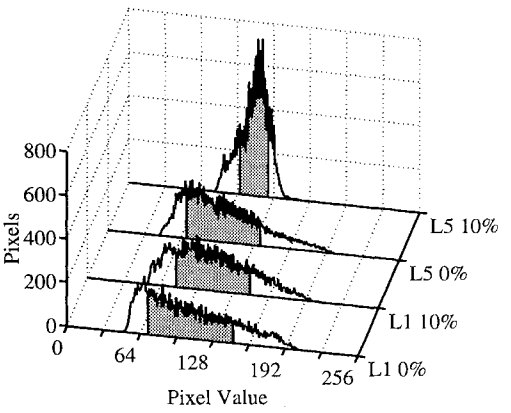

Fig. 1 Gray-scale histograms of a uniform-flow region for both single-slit (L1) and five-slit (L5) schlieren systems with spurious density gradients input at the test section (0%) and at 10% of the distance from the test section to the mirror.

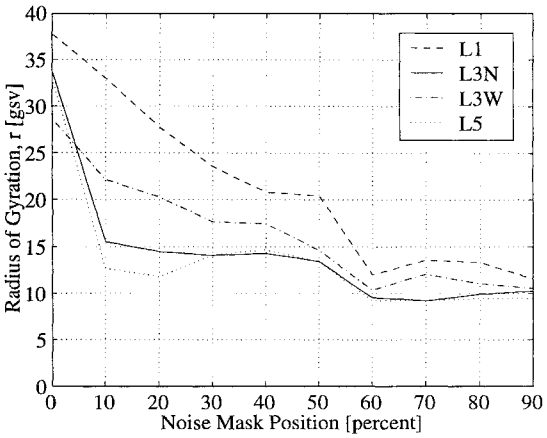

Fig. 2 Reduced sensitivity to spurious density gradients as measured by the radius of gyration of gray-scale histograms (L1, L3N, L3W, and L5 grids).

Note the slight deviation in all of the curves in Fig. 2 between the 50 and 60% marks. In this region of the system, the speckle mask enters the beam path twice, once while in the beam traveling to the second focusing mirror and again in the beam reflecting back to the cutoff grid. Through this region and beyond, previous analytical predictions[1] fail and measurements such as those presented here are required.

To quantify shock wave visibility, the rms values for the deviation of the intensity peaks of the shock waves are computed. This rms measure correlated well with observations of images; the shocks are visible in all cases. Hence, the data are not presented, though they are available in Ref. 10.

Conclusions

A single numerical measure of noise reduction, computed from the gray-scale histogram, appears to correlate well with visual observation of the images. It is shown that simple multiple-source modifications to an existing conventional schlieren system are a practical means of reducing the sensitivity of the system to spurious density gradients, typically, thermal currents outside the test section. Currents closest to the test section may fail to be attenuated significantly, depending on the integration length of the system. Thus, image noise generated by turbulent boundary layers or scratches on the test section windows are more difficult to alleviate than that from a drafty room.

Trends predicted by previous analysis are supported by the present experiments. Knowledge of noise reduction as measured for uniform flow regions and for shock visibility allows the effective design of multiple-source schlieren systems with desired amounts of noise reduction.

Experimental results for a system with f/10 spherical mirrors used 5 deg off axis demonstrate that the practical maximum grid size is approximately 15% of the mirror diameter. Regardless, the results show that simple modifications (only three to five slits) to existing mirrored schlieren systems can improve the quality of images originally obscured by the effects of spurious density gradients outside of the wind tunnel.

Acknowledgments

This research was supported through the 1992 U.S. Air Force Office of Scientific Research (AFOSR) Summer Faculty Program, and the 1993 AFOSR Summer Research Extension Program, Subcontract 93-144. Technical supervision was provide by George Seibert of Wright Laboratories.

References

[1]Collicott, S. H., and Salyer, T. R., "Noise Reduction Properties of a Multiple-Source Schlieren System," *AIAA Journal*, Vol. 32, No. 8, 1994, pp. 1683–1688.

[2]Settles, G. S., Hacket, E. B., Miller, J. D., and Weinstein, L. M., "Full-Scale Schlieren Flow Visualization," *Flow Visualization VII*, Proceedings of the 7th International Symposium on Flow Visualization (Seattle, WA), 1995, pp. 2–13.

[3]Burton, R. A., "A Modified Schlieren Apparatus for Large Areas of Field," *Journal of the Optical Society of America*, Vol. 39, Nov. 1949, pp. 907, 908.

[4]Kantrowitz, A., and Trimpi, R. L., "A Sharp-Focusing Schlieren System," *Journal of the Aeronautical Sciences*, Vol. 17, No. 5, 1950, pp. 311–314.

[5]Fish, R. W., and Parnham, K., "Focusing Schlieren Systems," Aeronautical Research Council, TR IAP 999, Nov. 1950.

[6]Boedeker, L. R., "Analysis and Construction of a Sharp Focusing Schlieren System." M.S. Thesis, Dept. of Aeronautics and Astronautics, Massachusetts Inst. of Technology, Cambridge, MA, May 1959.

[7]Weinstein, L. M., "Large-Field High-Brightness Focusing Schlieren System," *AIAA Journal*, Vol. 31, No. 7, 1993, pp. 1250–1255.

[8]Price Cook, S., and Chokani, N., "Quantitative Results from the Focusing Schlieren Technique," AIAA Paper 93-0630, Jan. 1993.

[9]Gartenberg, E., Weinstein, L. M., and Lee, E. E., Jr., "Aerodynamic Investigation wigh Focusing Schlieren in a Cryogenic Wind Tunnel," AIAA Paper 93-3485, Aug. 1993.

[10]Salyer, T. R., "Quantitative Noise Reduction Measurements of a Multiple-Source Schlieren System," M.S. Thesis, School of Aeronautics and Astronautics, Purdue Univ., West Lafayette, IN, May 1994.

[11]Collicott, S. H., "Evaluation of Options for Improved Large Grid Multiple-Source Schlieren Systems," AIAA Paper 94-2301, June 1994.

Drag of Freely Rotatable Cylinder/Splitter-Plate Body at Subcritical Reynolds Number

John M. Cimbala and Jonathan Leon
Pennsylvania State University,
University Park, Pennsylvania 16802-1412

Introduction

ROSHKO[1] was the first to show that attachment of a splitter plate to the back of a circular cylinder reduces the strength of shed vortices. Later, Bearman[2] showed that the addition of a splitter plate to the back of various kinds of bluff bodies could lead to significant reduction in body drag. Apelt and co-workers[3,4] conducted drag measurements on circular cylinders with splitter plates of various lengths; they showed that drag coefficient C_D decreased in general as splitter-plate length increased, except near $L/D = 2$, where the drag increased slightly. In all of these experiments, the splitter plates were rigidly mounted to the body at 0-deg angle of attack with respect to the freestream. The shortcoming of using rigidly mounted splitter plates is that flow in natural environments is rarely unidirectional. In engineering applications involving flow over a circular cylinder, such as offshore oil rigs, smokestacks, ocean thermal energy conversion systems, and five-hole probe measurements in three-dimensional flowfields, the direction of the freestream flow is not known a priori. Such applications would benefit greatly if the splitter plate could rotate freely, aligning itself with the flow direction. Cimbala and co-workers[5,6] studied the flow over a freely rotatable cylinder/splitter-plate body, hoping to attain similar benefits (i.e., reduction in the drag and the strength of shed vortices) as are attained with fixed splitter plates, but with the additional benefit of being omnidirectional. What they found was somewhat surprising: The freely rotatable splitter plate does not align itself with the freestream flow direction, but rather rotates to some nonsymmetric equilibrium position at an angle θ with respect to the freestream direction. (The equilibrium angle could, of course, be positive or negative with equal probability.) They measured this equilibrium angle as a function of L/D, the ratio of splitter-plate length to cylinder diameter, and found that θ decreased from nearly 90 deg for very small splitter-plate lengths to 0 deg for large splitter plates ($L/D > 5$), as shown in Fig. 1 of Ref. 6.

Cimbala and Garg[6] measured wake profiles downstream of cylinders both with and without splitter plates, and for cases with the splitter plate either rigidly attached at 0 deg or free to rotate. They also obtained smoke-wire photographs of these wakes. When L/D was less than about 2, the wake of the freely rotatable cylinder/splitter-plate body was not significantly altered by the presence of the plate, but the fixed splitter plate altered the wake significantly. However, splitter plates larger than about two cylinder diameters had nearly the same effect on the wake of the cylinder regardless of whether rigidly attached or free to rotate. Drag was not measured in these earlier experiments.

Since the discovery of this nonsymmetric behavior of freely rotatable cylinder/splitter-plate bodies, Xu et al.[7,8] have done extensive numerical analyses to help explain the phenomenon. Most importantly, they predicted a critical Reynolds number below which the cylinder/splitter-plate body remains at 0-deg angle of attack and above which it becomes unstable and rotates to its nonsymmetric orientation. The Reynolds number at which this bifurcation occurs

Received March 25, 1996; revision received May 20, 1996; accepted for publication May 31, 1996; also published in *AIAA Journal on Disc*, Volume 1, Number 4.

*Associate Professor, Department of Mechanical Engineering. Member AIAA.

†Undergraduate Assistant, Department of Mechanical Engineering; currently Engineer, Engineering Department, Voith Hydro, Inc., York, PA 17405.